Fenton-like oxidative degradation of Orange G dye and binary dye mixtures using Oxone® activated with cobalt-doped alumina catalysts

Sanja R. Marinović[1], Tihana M. Mudrinić[1], Marija J. Ajduković[1], Nataša P. Jović-Jovičić[1], Dimitrinka A. Nikolova[2], Predrag T. Banković[1] and Tatjana B. Novaković[1]

[1]*University of Belgrade - Institute of Chemistry, Technology and Metallurgy, Department of Catalysis and Chemical Engineering, Belgrade, Serbia*

[2]*Institute of Catalysis, Bulgarian Academy of Sciences, Sofia, Bulgaria*

Abstract

Two texturally and structurally different Co-doped aluminas were obtained by using the sol-gel method followed by calcination at temperatures of 1000 °C and 1100 °C. The obtained materials were tested as catalysts in anionic textile dye Orange G (OG) degradation using Oxone® as a precursor of sulfate anion radicals, the main reactive oxygen species. Effects of temperature and initial pH on degradation efficiency was investigated. The increase in temperature accelerated the reaction rate and the maximal degradation efficiency was obtained at 60 °C. Different kinetic models were applied and pseudo-first order rate was found to be the most appropriate. Both catalysts showed the optimal performance in the pH range around neutral. Coexisting cations (Ca^{2+}, Mg^{2+}, K^+ and Na^+) enhanced the OG degradation rate, as well as anions: Cl^- and $H_2PO_4^-$, while NO_3^-, $SO_4^{2-}$and HCO_3^- inhibited the degradation. The catalysts were also proved effective in degradation of the other investigated dyes: Methylene blue, Basic blue 41, and Remazol brilliant blue R. Finally, simultaneous degradation of OG in binary dye mixtures was investigated showing that the synthesized catalysts can be also used in simultaneous processes of dye degradation. However, differences in structural and textural properties of the two catalysts affected their catalytic performance.

Keywords: Sol-gel alumina; anionic and cationic dyes, peroxymonosulfate; advanced oxidation processes; simultaneous dye degradation.

Available on-line at the Journal web address: http://www.ache.org.rs/HI/

ORIGINAL SCIENTIFIC PAPER

UDC: 667:778.665

Hem. Ind. **78(4)** 359-370 (2024)

1. INTRODUCTION

Aluminum (III) oxide, often called “alumina” belongs to the group of surface-active metal oxides [1]. The synthesis method used to obtain aluminas affects the surface properties of the synthesized material. Sol-gel method is one of the often-used preparation methods by which the structural and textural properties of aluminas can be altered in a desired manner. By synthesizing alumina with specific physicochemical properties its catalytic activity can be controlled [2,3]. Several metastable crystalline structures of alumina can be obtained: η-, γ-, δ-, θ-, β-, κ-, χ, and α-alumina (thermodynamically most stabile phase) [4], while by rising the calcination temperature one phase will transform to another. At calcination temperatures above 800 °C, γ-Al_2O_3 transforms to δ-Al_2O_3 followed by further transformation to θ-Al_2O_3 above 1000 °C, and above 1100 °C the α- Al_2O_3 phase is obtained [5]. Yet, if the impurities are present, the phase transformation temperatures will be altered [4]. Therefore, a material with desired properties can be designed by doping alumina with different metals, which changes the properties of the new surface compared to the parent alumina. Metal-doped aluminas have shown good potential as adsorbents and catalysts in wastewater treatments to remove different organic pollutants [6,7]. This is important as removal of organic pollutants is often not possible by conventional processes and therefore, oxidative degradation using Fenton-like processes is more applicable [8,9,10]. To the best of our knowledge, using transition metal-doped aluminas as catalysts in catalytic oxidative degradation of organic

Corresponding authors: Sanja R. Marinović, University of Belgrade - Institute of Chemistry, Technology and Metallurgy, Department of Catalysis and Chemical Engineering, Njegoševa 12, 11000 Belgrade, Republic of Serbia

Paper received: 26 January 2023; Paper accepted: 17 August 2024; Paper published: 26 August 2024.

E-mail: sanja.marinovic@ihtm.bg.ac.rs

https://doi.org/10.2298/HEMIND240126016M

pollutants in wastewater in the presence of Oxone® was first investigated by our research group [7]. We have investigated degradation of the food dye Tartrazine using three alumina catalysts with different crystalline structures and different textural properties. Oxone® was used as a source of sulfate anion radicals, proven to be superior to hydroxyl radicals in Fenton-like processes for degradation of different organic pollutants [11,12].

Apart from food dyes, textile dyes, are often found in industrial wastewaters. The textile industry produces large amounts of wastewater containing genuine reactive textile dyes [13,14]. One of the representatives, and often used textile dyes is Orange G (OG). OG is a synthetic acidic azo-dye, which is toxic and non-biodegradable [15]. Due to its high solubility in water, OG can be present in wastewater from textile, leather, and printing industries at high concentrations. Given OG's potentially carcinogenic nature, it is a high priority to find an efficient way for removal from wastewater [16]. Since Co-doped alumina catalysts (CoA) tested in Tartrazine degradation showed excellent performance, two selected catalysts with different alumina phases and different textural properties were investigated in this work for catalytic OG degradation in the presence of Oxone®. The first catalyst labeled CoA-1000 was calcined at 1000 °C containing the γ-Al_2O_3phase. On the other hand, the second catalyst labeled CoA-1100 calcined at 1100 °C has shown the presence of α- Al_2O_3. Several reaction parameters were investigated to determine the effects of different material structures and properties on the catalytic performance in Oxone® induced OG dye degradation. Apart from OG degradation, simultaneous degradation of OG and three other dyes: Methylene blue, Remazol brilliant blue R, and Basic blue 41 were tested to get an insight in the interactions of different dyes and to assess if the catalyst efficiency changes in a complex system.

2. EXPERIMENTAL

2. 1. Materials and synthesis

Oxone® (potassium triple salt - $KHSO_5 \cdot 0.5 \cdot KHSO_4 \cdot 0.5 \cdot K_2SO_4$), Orange G (OG), Methylene blue (MB), Remazol brilliant blue R (RB), Basic blue 41 (BB), NaCl (*p.a.*), $NaHCO_3$ (*p.a.*), $NaNO_3$ (*p.a.*), Na_2SO_4 (*p.a.*), $NaH_2PO_4 \cdot H_2O$ (*p.a.*), KCl (*p.a.*), $CaCl_2$ (anhydrous >98 %), and $MgCl_2$ (anhydrous >98 %), were supplied by Sigma Aldrich (USA) and were used as received. Structural formulas of the dyes are presented in Figure S1 (Supplementary material).

Two Co-doped alumina catalysts were synthesized using the sol-gel method and calcined at 1000 °C (CoA-1000) and 1100 °C (CoA-1100). The synthesis and characterization of the synthesized materials were presented previously [7]. In addition to previous characterization, the morphology of both catalysts was studied using scanning electron microscopy with energy dispersive spectroscopy (SEM-EDS). The samples were characterized by a dual beam scanning electron/focused ion beam system (SEM/FIB LYRA I XMU, TESCAN, Czech Republic), equipped with an EDX detector (Quantax 200, Bruker, Germany). SEM-EDS analyses were performed under the following conditions: tungsten filament, resolution: 3.5 nm at 30 kV, accelerating voltage: 200 V - 30 kV, EDX detector: spectroscopic resolution at Mn-Kα was 126 eV. The maximum input count range was 1 kcps.

2. 2. Catalytic tests

In all catalytic tests, 200 cm^3 of aqueous solution of a dye was introduced into a thermostated Pyrex reactor. The stirring was provided by a mechanical stirrer. After reaching the desired reaction temperature, 1 cm^3 of Oxone solution (40 mg of Oxone®) was added to the dye solution, and 10 mg of catalyst was added right after that initial moment (0 min of the reaction). The aliquots (2 cm^3) were taken at predetermined time intervals after the reaction started. Supernatant solutions were separated from the catalyst by centrifugation. Degradation of dyes was determined by measuring the decrease in the peak maximum at 478 nm, for OG, and at 665, 592 and 609 nm for MB, RB, and BB respectively, using UV-Vis spectrophotometry (Evolution 220, Thermo Scientific, USA).

For OG, the effects of temperature and the initial pH on the degradation efficiency were monitored. The starting OG concentration was 50 mg dm^{-3} in all experiments. The effect of temperature was investigated in the range from 30 °C to 60 °C at unadjusted pH 3.7 and the effect of the initial pH was followed in the pH range 2 to 9, at 30 °C. The experimentally obtained data were modeled by the zero, pseudo-first, and pseudo-second order kinetic models in order to determine reaction kinetics.

Prior to catalytic tests, the adsorption of each of the dyes on the CoA-1000 and CoA-1100 as adsorbents was examined, without the presence of Oxone®, and the amount of adsorbed dyes was less than 3 %. Degradation of OG with Oxone® without a catalyst under the same experimental conditions was negligible meaning that the presence of a catalyst for Oxone® activation was necessary.

To examine the influence of coexisting anions and cations, each ion was added (as a water-soluble salt) to the OG solution ($C_{0,OG}$ = 50 mg dm^{-3}), so that the concentration of that ion in the dye solution was 5 mmol dm^{-3}. For investigations of the effects of Cl^- and NO_3^- ions, additional experiments were performed with the ion concentration of 20 mmol dm^{-3}. In all these experiments, the reaction temperature was 50 °C and the CoA-1000 catalyst was used. All other experimental conditions were the same as stated above.

For experiments using MB, RB, and BB, the starting dye concentration was 20 mg dm^{-3} in single dye experiments. In binary system degradation experiments, 20 mg dm^{-3} of each dye was applied. The degradation degree of investigated dyes was calculated by comparing the absorbance at the characteristic wavelengths at predefined reaction times with the initial absorbance values. In these experiments, the reaction temperature was 30 °C.

3. RESULTS AND DISCUSSION

The catalysts' characterization results were previously published [7]. However, an overview of the structural, phase and textural properties of the catalysts is presented here to facilitate the interpretation of the obtained results.

The X-ray powder diffraction (XRPD) analysis confirmed that the main phase in both catalysts was some type of Co-spinel (Co_3O_4, $CoAl_2O_4$, Co_2AlO_4), and the second phase was identified to be γ-Al_2O_3 stabilized by cobalt for CoA-1000, and α-Al_2O_3 for CoA-1100. H_2-temperature programmed reduction (H_2-TPR) confirmed the presence of Co_3O_4/$CoAl_2O_4$ in CoA-1000, and $CoAl_2O_4$ in CoA-1100. Using the N_2 physisorption technique textural parameters of synthesized catalysts were obtained. The specific surface area of the CoA-1000 (S_{BET} = 43 m^2 g^{-1}) was over 4 times higher than that of CoA-1100 (S_{BET} = 10 m^2 g^{-1}). Similar results were observed for the total pore volume ($V_{0.98}$ = 0.122 cm^3 g^{-1} for CoA-1000, and $V_{0.98}$ = 0.057 cm^3 g^{-1} for CoA-1100) [7].

In this paper, the morphology of CoA-1000 and CoA-1100 catalysts was examined using the SEM-EDS characterization technique. The surface chemical composition of catalysts is presented in Table 1. The analysis of the results revealed enrichment of the CoA-1100 catalyst surface with cobalt by 7 % as compared to that of CoA-1000. At the same time, a decrease in surface oxygen concentration is observed for CoA-1100. Calculation of the Co/Al mass ratio and EDS element mapping, for the same image of magnification used for quantity control, confirmed differences between the two catalysts (Figs. 1a, 1d, 2a, and 2d). These observations are in accordance with different phase structures of CoA-1000 and CoA-1100. It is obvious that the complete formation of $CoAl_2O_4$ during calcination at 1100 °C led to an increase in cobalt distribution on the surface.

Table 1. Surface chemical compositions of CoA-1000 (in Fig. 1a) and CoA-1100 (in Fig. 2a)

Sample	Surface concentration, wt.%			Co/Al mass ratio
	O	Al	Co	
CoA-1000	30.87	32.04	37.09	1.16
CoA-1100	25.72	30.08	44.20	1.47

The images of selected areas at higher magnifications showed very different morphology of the two catalysts (Figs. 1b, 1c, 2b, and 2c). The surface microstructure of the CoA-1000 catalyst is characterized by plate-like formations of different sizes and the presence of white spherical particles of similar sizes. These results are consistent with the findings from low-temperature N_2 physisorption. The obtained morphology of CoA-1000 corresponds to aggregated planar particles and slit type pores [7]. The presence of Co_3O_4/$CoAl_2O_4$ phases at the CoA-1000 surface is also recognized indirectly by the EDX technique. The increase in the calcination temperature of 100 °C led to more homogeneous morphology and plate formation was not observed in the case of the CoA-1100 catalyst. The agglomeration of spherical particles was observed for CoA-1100 as well as for CoA-1000. However, CoA-1100 exhibited a more pronounced effect when observed at higher magnification (Fig. 2c). Comparison of EDS mapping images of Co for both catalysts (Figs. 1f and 2f) reveals the enrichment of cobalt on the CoA-1100 surface.

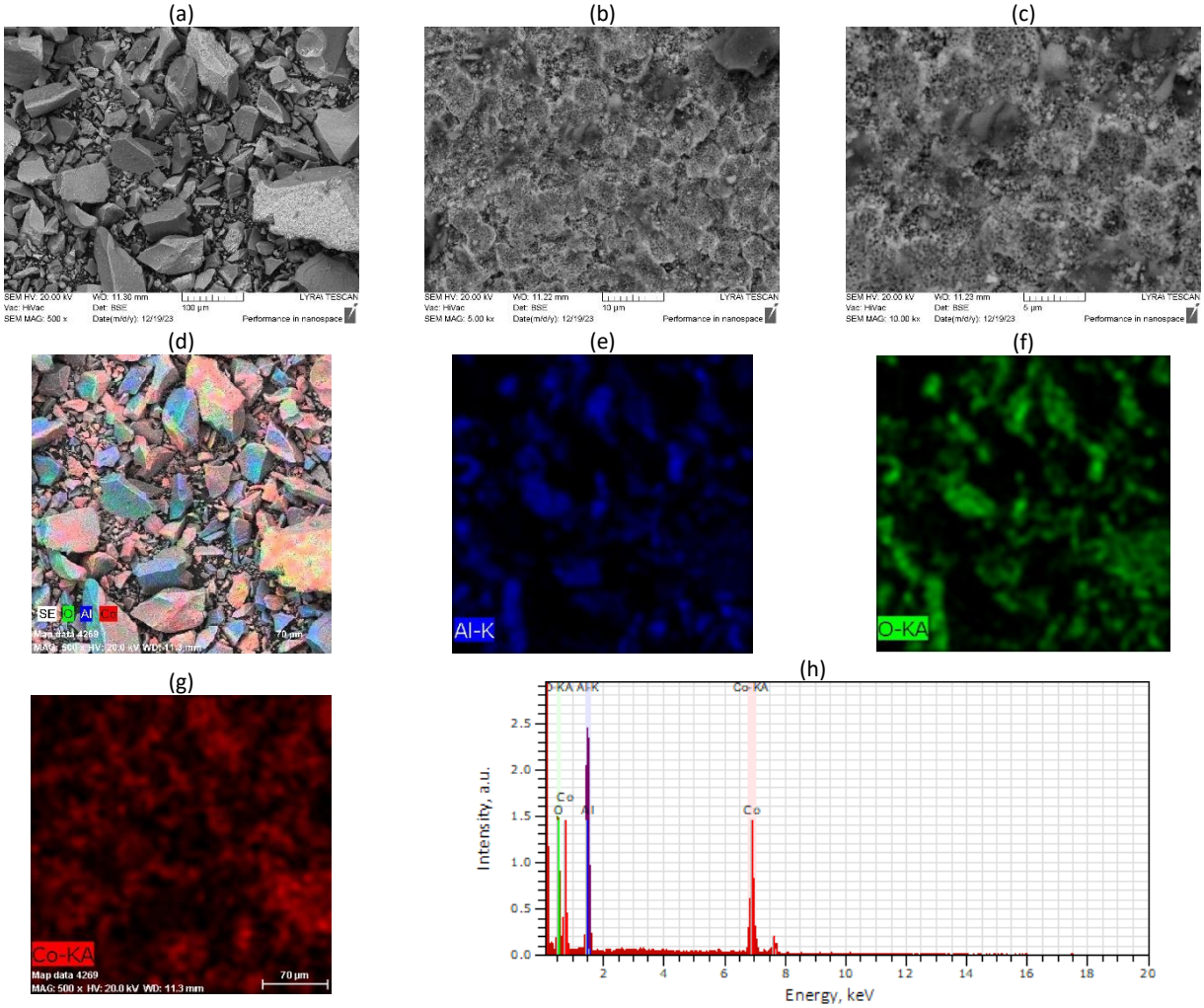

Figure 1. SEM images of CoA-1000: a-c - different magnifications; d-g - EDS elemental mapping of Co, Al, O; h - EDX spectrum determined for the image a

3. 1. Catalytic tests

3. 1. 1. Influence of temperature

The influence of temperature on the catalytic degradation of the OG was investigated for 120 min in the temperature range from 30 °C to 60 °C. The reaction extent was followed by measuring the characteristic OG's UV adsorption peak at 478 nm originating from the azo group in the OG molecule. With the increase in the reaction temperature, the degradation rate increased, as expected, being significantly higher for CoA-1000 (Fig. 3a) as compared to that for CoA-1100 (Fig. 3b) at all investigated temperatures. The OG dye was completely degraded after 120 min in the presence of CoA-1000 at temperatures above 45 °C. On the other hand, for CoA-1100, the complete degradation was achieved only at 60 °C in the investigated period. The proposed degradation mechanism for the catalyst CoA-1000 at the temperature of 60 °C is presented in Chapter S3 (Supplementary material).

Zero (Eq. (1)), pseudo-first (PFO) (Eq. (2)), and pseudo-second order (PSO) (Eq. (3)) kinetic models in linear forms were applied to the obtained experimental data (Fig. 4 for PFO and Figs S2-S5 for zero and PSO models in Supplementary material).

$$C_t = C_0 - k_0 t \quad (1)$$

$$\ln C_t = \ln C_0 - k_1 t \quad (2)$$

$$1/C_t = 1/C_0 + k_2 t \quad (3)$$

C_t is the dye concentration in aqueous solution at any time t, C_0 is the starting dye concentration, and k_0, k_1, and k_2 are zero, pseudo-first, and pseudo-second order rate constants respectively.

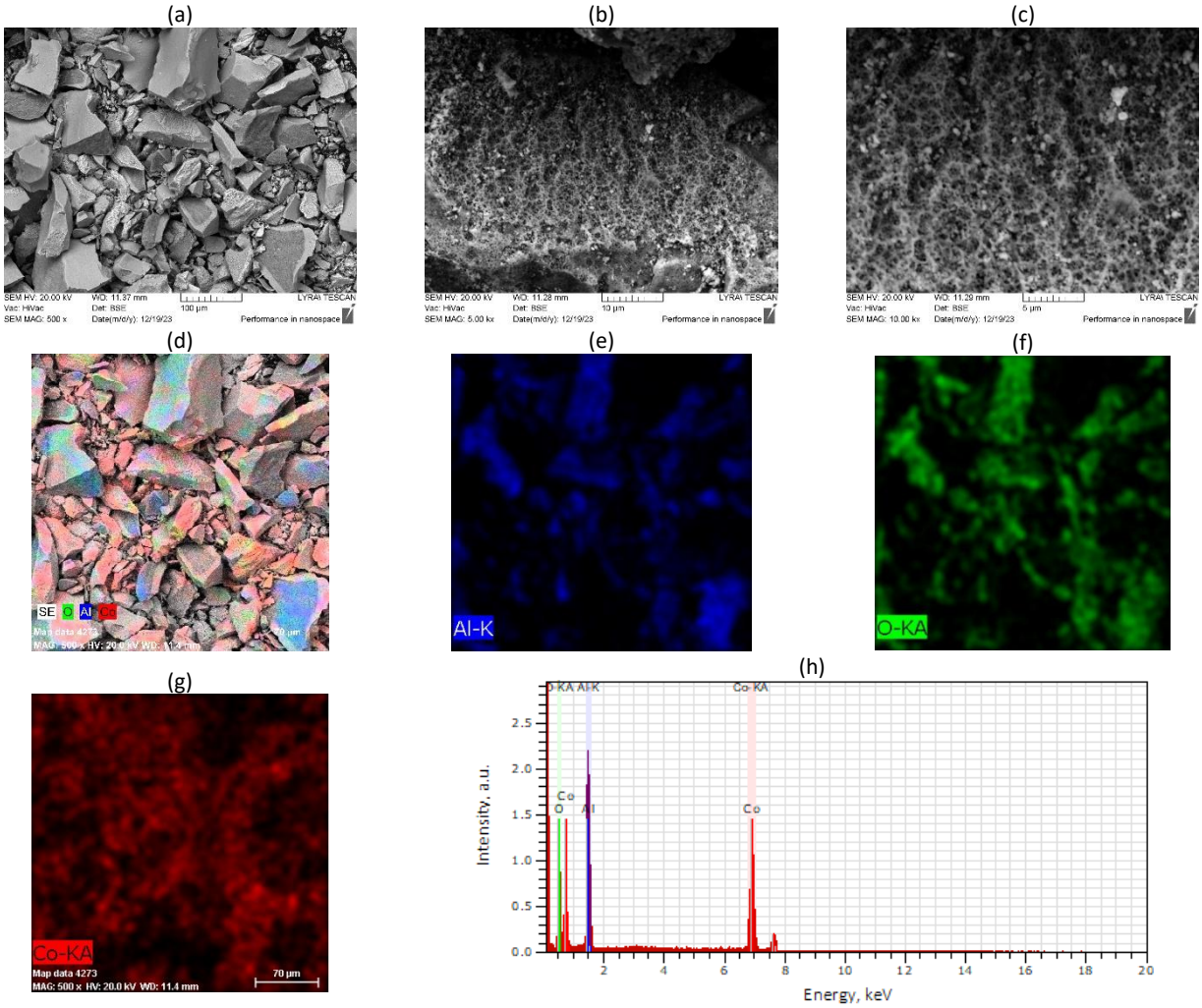

Figure 2. SEM images of CoA-1100: a-c - different magnifications; d-g - EDS elemental mapping of Co, Al, O; h - EDX spectrum determined for the image a

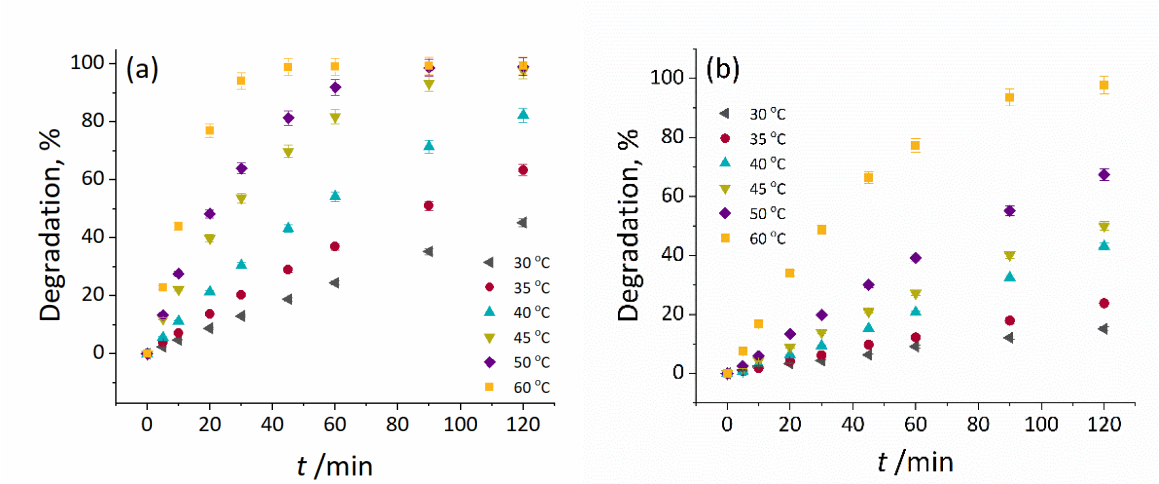

Figure 3. Influence of the temperature on the OG degradation extent for: a) CoA-1000 and b) CoA-1100 ($C_{0,OG}$ = 50 mg dm^{-3}; $V_{OGsolution}$ = 200 cm^3; $m_{Oxone®}$ = 40 mg; m_{cat} = 10 mg)

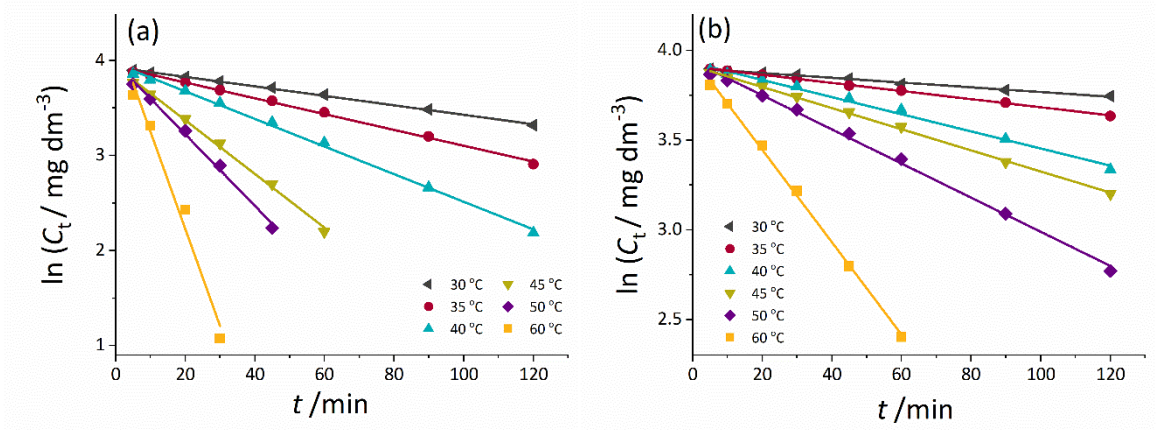

Figure 4. Application of the PFO kinetic model (lines) on experimental data (symbols) for OG degradation at different temperatures for:(a) CoA-1000 and (b) CoA-1100 ($C_{0,OG}$ = 50 mg dm^{-3}; $V_{OGsolution}$ = 200 cm^3; $m_{Oxone®}$ = 40 mg; m_{cat} = 10 mg).

For lower temperatures, both zero and PFO showed good agreement between experimental data and applied models, with slightly better fitting obtained with the PFO model. At higher temperatures, it becomes evident that the PFO kinetic model aligns better with the experimental data. The PSO model did not fit the data well, as expected. This trend is also noticeable when comparing kinetic model parameters shown in Table 2.

Table 2. Kinetic model parameters

			Temperature, °C					
Catalyst	Kinetic model		30	35	40	45	50	60
CoA-1000	Zero	k_0×10^2 / mg dm^{-3} min^{-1}	18.75	24.79	33.93	52.16	82.81	139.50
		R^2	0.9982	0.9941	0.9709	0.9082	0.9783	0.9700
	Pseudo-first	k_1×10^2 / min^{-1}	0.50	0.83	1.45	2.83	3.77	10.22
		R^2	0.9984	0.9975	0.9972	0.9968	0.9953	0.9802
	Pseudo-second	k_2×10^2 / dm^3 mg^{-1} min^{-1}	0.01	0.03	0.08	0.11	0.2	1.22
		R^2	0.9852	0.9657	0.9272	0.9673	0.9253	0.8355
CoA-1100	Zero	k_0×10^2 / mg dm^{-3} min^{-1}	6.21	9.90	18.01	20.97	28.16	64.68
		R^2	0.9901	0.9985	0.9989	0.9964	0.9906	0.9795
	Pseudo-first	k_1×10^2 / min^{-1}	0.13	0.23	0.48	0.59	0.95	2.58
		R^2	0.9932	0.9991	0.9923	0.9987	0.9970	0.9985
	Pseudo-second	k_2×10^2 / dm^3 mg^{-1} min^{-1}	0.003	0.005	0.010	0.020	0.030	0.110
		R^2	0.9932	0.9967	0.9739	0.982	0.9591	0.9421

R^2 - square of coefficient of correlation; k- rate constants

Although at lower temperatures, especially for CoA-1100, R^2 values for zero and for PFO are similar, small differences in favor of PFO are noticeable. This behavior is expected and reported in similar systems, where even a zero kinetic model is more applicable at lower temperatures. PFO is expected to be the best fit for the experimental data because Oxone® is present in great excess.

To check whether the application of the kinetic models in linear and non-linear forms fit the data equally well, the data were also fitted with the PFO model in non-linear form. The obtained kinetic parameters for the PFO model applied in the nonlinear form are presented in Table S1 in Supplementary material. Application of the PFO model in both linear and non-linear forms provided very similar results confirming that in the present case, linear fitting was sufficiently good. PFO rate constants (k_1) increased with increasing the reaction temperature for both catalysts. The k_1 values for CoA-1000 were more than 3 times higher than for CoA-1100, for all investigated temperatures, leading to the conclusion of higher catalyst efficiency of CoA-1000. The differences in textural and structural characteristics between CoA-1000 and CoA-1100 can explain the differences in their activity as catalysts in investigated reactions. The textural properties of CoA-1000 were much better compared to CoA-1100, with four times higher specific surface area, and twice as high the total pore volume. Also, the presence of the *γ*-alumina phase in CoA-1000, stabilized with a small amount of cobalt, provided more accessible active sites leading to higher activity of this catalyst. But the most important feature of CoA-1000

is the presence of Co_3O_4 which is much more active in Oxone® activation reaction than $CoAl_2O_4$ (the only Co phase identified in CoA-1100) where cobalt is strongly attached to the alumina matrix making it harder to promote Oxone® activation [7].

To calculate activation energy (E_a / J mol^{-1}), obtained pseudo-first order rate constants were applied in the Arrhenius equation (Eq. 4):

$$\ln k_1 = \ln A - \frac{E_a}{RT} \quad (4)$$

A: constant related to the geometry; *T* / K: thermodynamic temperature and *R*: universal gas constant (8.314 J / mol^{-1} K^{-1}).

From the ln k_1 *vs.* T^{-1} plot (Fig. 5) activation energy was calculated.

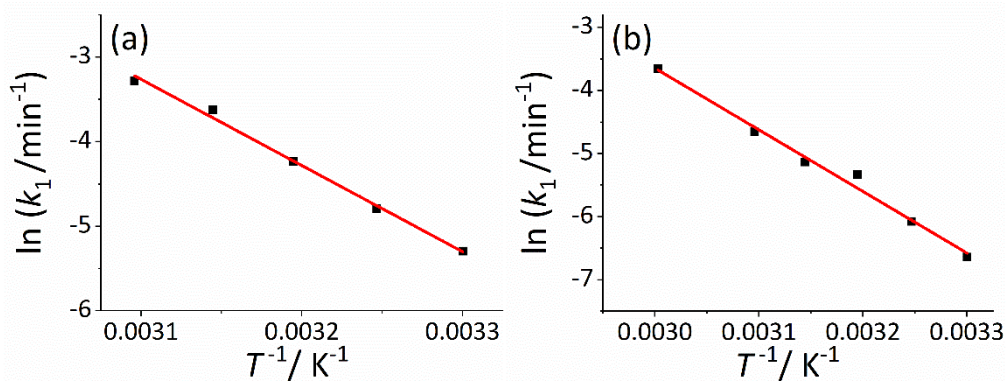

Figure 5. Arrhenius plot for the degradation of OG using a) CoA-1000 and b) CoA-1100 as catalyst

E_a was found to be 82.98 kJ mol^{-1} and 81.28 kJ mol^{-1} for CoA-1000 and CoA-1100 respectively. These values are of the same order of magnitude as those reported in the literature for OG degradation in the presence of sulfate ion radicals [16,17].

3. 1. 2. Influence of pH

The influence of the pH of the initial solution (pH_i) on the degradation of OG was investigated for different pH_i from 2 to 9 for both investigated catalysts. The unadjusted initial pH value of pH_i 3.7 was included in these graphs. In Figure 6 degradation of OG at different initial pH values is shown.

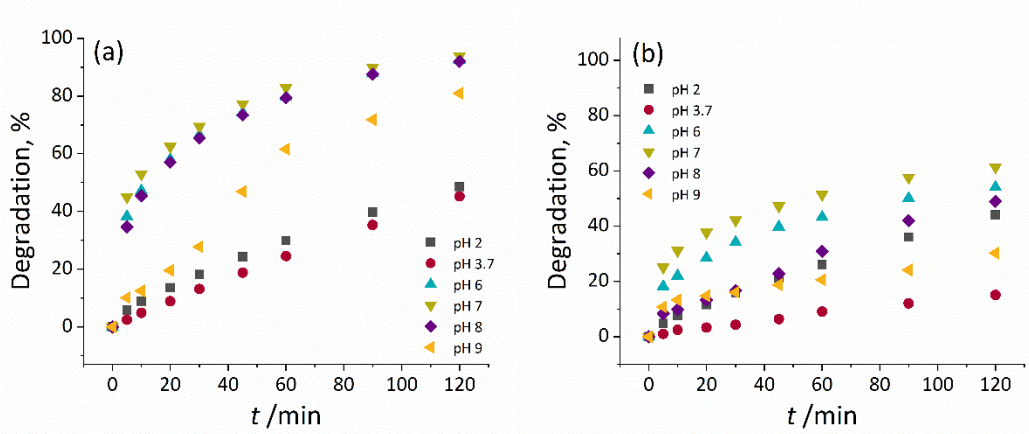

Figure 6. Degradation of OG monitored at different initial pH values for a) CoA-1000 and b) CoA-1100 ($C_{0,OG}$ = 50 mgdm^{-3}; $V_{OG\ solution}$ = 200 cm^3; $m_{Oxone®}$ = 40 mg; m_{cat} = 10 mg; θ = 30 °C)

The highest degradation rate was obtained for pH_i 7, for both catalysts. For CoA-1000 for pH_i 6-8, reaction rate was almost the same, and more than 90 % of degradation was achieved after 120 min of the reaction. On the other hand, for CoA-1100, differences in reaction rate were more pronounced in this pH_i range. After 120 minutes, the highest degradation of 60 % was obtained at pH_i 7. At pH_i 8 the reaction was slow at the beginning, and then it became faster

reaching 45 % of degradation at the end. Similar behaviour was obtained for Tartrazine degradation using investigated catalyst [7]. For all pH_i the degradation of OG for CoA-1100 was much lower than for CoA-1000.

3. 1. 3. The effect of coexisting ions

Since real wastewater usually contains various inorganic ions, it is important to investigate their effect on OG degradation efficacy in the presence of Oxone®, as these ions can interfere with the activation of Oxone®. In this work, the effects of the most common anions: Cl^-, HCO_3^-, NO_3^-, SO_4^{2-}, and $H_2PO_4^-$ on OG degradation were investigated. Apart from anions, the effect of cations K^+, Mg^{2+}, and Ca^{2+} was also tested. The tests were performed at 50 °C to allow better monitoring of the change in the absorbance peak at 478 nm and because complete decolorization was achieved after 60 min only at that temperature. The concentration of the added anion (in water solution) was 5 mmol dm^{-3}, chosen in accordance with the literature as well as the estimation of concentrations in the real water [18,19,20]. For $Cl^-$and NO_3^- anions an additional higher concentration (20 mmol dm^{-3}) was also investigated to confirm the influence of these species. The results are presented in Figure 7 (*i.e.* effects of anions and cations are presented in Fig. 7a and 7b, respectively).

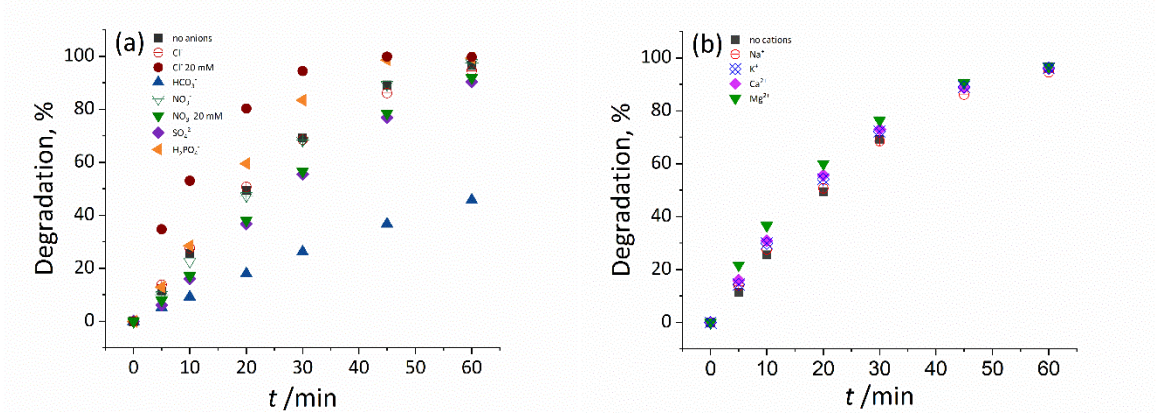

Figure 7. Influence of the coexisting ions on degradation of OG for CoA-1000 catalyst: (a) effects of anions, (b) effects of cations ($C_{0,OG}$ = 50 mg dm^{-3}; $V_{OG\ solution}$ = 200 cm^3; $m_{Oxone®}$ = 40 mg; $m_{CoA-1000}$ = 10 mg; θ = 50 °C)

It is noticeable that some anions speed up and others slow down the degradation of OG, while all the investigated cations had a positive effect on the reaction rate. The experiments showed that HCO_3^- had the most significant influence on OG degradation causing a decrease in the reaction rate of approximately 2.5 times. Only 45 % of degradation was achieved after 60 min, while in the system without the added ions almost complete degradation was observed at the same reaction time. This phenomenon is expected according to literature, since the HCO_3^- can scavenge free radicals and impede the degradation process by generating carbonate radical ($CO_3^{\cdot-}$), which has a lower oxidation ability [18,19,21]. Still, it can react with $SO_4^{\cdot-}$ and $HO^{\cdot}$ leading to lowering their concentrations in the reaction system. Sulfate anions (SO_4^{2-}) have also suppressed degradation of OG but for the investigated concentration this effect was less pronounced than that observed for HCO_3^-. Since SO_4^{2-} is produced in one of the steps of Oxone® decomposition, the existence of SO_4^{2-} in the system will inhibit the formation of SO_4^{2-} from HSO_5^- by reducing the formation of reactive species $SO_4^{\cdot-}$ [22]. On the other hand, $H_2PO_4^-$ showed an accelerating effect on reaction rate since these anions promote Oxone® degradation according to the literature [21,23]. Nitrate and chloride anions only slightly affected the reaction rate. Since the effect of these anions was not sufficiently clear for the investigated concentration of 5 mmol dm^{-3}, a higher concentration of 20 mmol dm^{-3} was also applied. It was concluded that NO_3^- anions inhibited OG degradation because they can rapidly react with $SO_4^{\cdot-}$ to form $NO_3^{\cdot}$ [20]. On the other hand, the enhancing effect of Cl^- ions on OG degradation was confirmed. This was in line with literature findings for similar systems, where even an inhibitory effect of Cl^- ions was found for very low concentrations such as 1 mmol dm^{-3}, but at higher concentrations, a promoting effect of these anions on the degradation process in Oxone® systems was reported [9,24,25,26]. It is assumed that chloride ions directly react with Oxone® to form active chlorine species that participate in dye degradation. Chloride ions can combine with hydroxyl radicals to generate chloride radicals whose oxidability is superior to hydroxyl radicals and even similar to sulfate ion radicals. This is the main cause of increasing the degradation efficiency by Cl^- ions.

The effect of non-redox metal cations Ca^{2+}, Mg^{2+}, K^{+}, and Na^{+} on the degradation of OG in the Co/Oxone® system was also studied by using 5 mmol dm^{-3} concentrations of aqueous solutions of chloride salts. The examined cations showed a slight influence on the reaction rate at the examined cation concentration. Still, it is clear that these cations have an accelerating effect that can be presented in the following sequence: $Na^{+}< K^{+}< Ca^{2+}< Mg^{2+}$. This suggests that the reaction rate increased with increasing the Lewis acidity of non-redox metal ions. Similar results were obtained by other authors [27].

It can be concluded that the effects of coexisting ions are complex. The overall effect of the coexistence of several ions in the Co/Oxone® system depends on many factors, such as the ion type, concentrations of each species, *etc*.

3. 1. 4. Simultaneous dye degradation

Since more than one pollutant is usually present in real wastewater, it was important to investigate the simultaneous degradation of dyes to see how their interaction changes the degradation efficiency.

Prior to simultaneous degradation tests, the degradation experiments of single dyes were performed under the same reaction conditions as in a binary mixture. The starting concentrations of dyes were 20 mg dm^{-3} for each dye in binary dye mixed solutions. Three combinations of two dyes systems were investigated: OG-MB, OG-RB, and OG-BB. The reaction time was extended to 240 min so that degradation of both dyes could be followed.

In Figures 8 and 9 the results obtained for degradation of single dyes are presented together with degradation efficiencies obtained for binary dye mixtures under the same experimental conditions using CoA-1000 and CoA-1100.

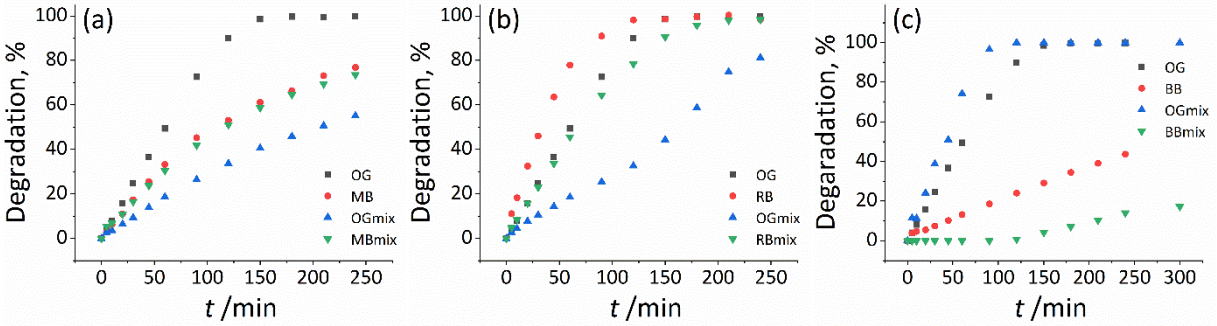

Figure 8. Degradation efficiency for single dyes and binary dye mixtures for CoA-1000 catalyst: (a) OG and MB, (b) OG and RB, and (c) OG and BB ($C_{0,dye}$ = 20 mg dm^{-3} ; $C_{0,dye\ mix}$ = 20 mg dm^{-3}; $V_{dye\ solution}$ = 200 cm^3 ; $m_{Oxone®}$ = 40 mg; $m_{CoA\text{-}1000}$ = 10 mg; θ = 30 °C).

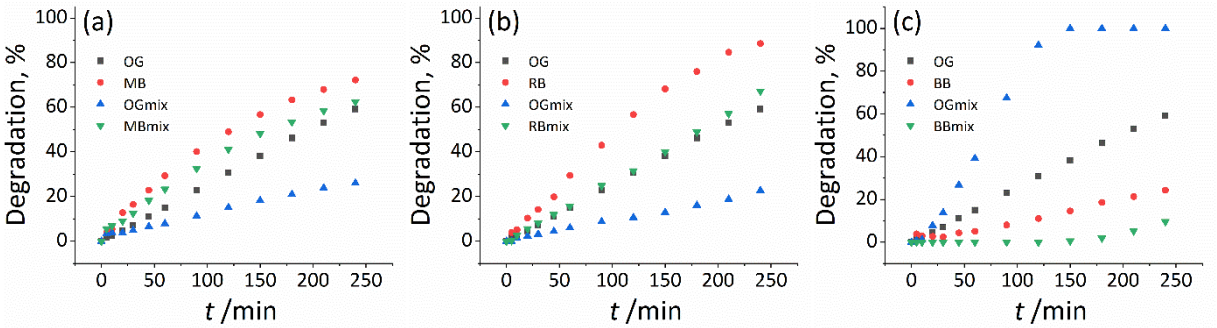

Figure 9. Degradation efficiency for single dyes and binary dye mixtures for CoA-1100 catalyst: (a) OG and MB, (b) OG and RB, and (c) OG and BB ($C_{0,dye}$ = 20 mg dm^{-3}; $C_{0,dye\ mix}$ = 20 mg dm^{-3}; $V_{dye\ solution}$ = 200 cm^3; $m_{Oxone®}$ = 40 mg; $m_{CoA\text{-}1100}$ = 10 mg; θ = 30 °C)

Differences in the results obtained for CoA-1000 and CoA-1100 are very pronounced. The efficiency of CoA-1100 was much lower for the degradation of single dyes and binary dye mixtures, but also the degradation profiles are noticeably different as compared to those obtained for CoA-1000.

For OG and MB combination of dyes, CoA-1000 was the most effective catalyst in OG single dye degradation, with complete degradation achieved after 150 min. In contrast, for MB as a single dye about 80 % of degradation was obtained during the entire investigated period. On the other hand, CoA-1100 was found to be the most effective in MB single dye degradation, achieving similar degradation of this dye as with CoA-1000 as the catalyst.

Degradation of OG (OG_{mix}) in the binary dye mixture with MB was significantly slower than in the single dye solution and compared to the MB_{mix} degradation for both catalysts, but with CoA-1000 the degradation percent of OG_{mix} was about twice as high as that obtained for CoA-1100. The effectiveness of MB_{mix} degradation with CoA-1000 as a catalyst was very similar to MB degradation in a single dye system, while for CoA-1100, degradation of the MB_{mix} was a bit lower.

In the OG and RB system, both catalysts had the best performance for RB single dye degradation, but the degradation rate of RB was significantly higher with CoA-1000. The complete degradation of this dye was achieved after 120 min for CoA-1000, while for CoA-1100 approximately 90 % degradation was reached after 240 min. When it comes to degradation in the binary dye mixture, a significantly higher rate was obtained for RB_{mix} for both catalysts. Degradation of OG and OG_{mix} was the slowest process for both investigated catalysts. Also, in the case of the CoA-1000 catalyst degradation of OG_{mix} has accelerated when most of the RB_{mix} amount was degraded.

In the OG and BB combination of dyes, the noticed behaviour was pronouncedly different than that observed in the other two systems. Firstly, both investigated catalysts showed selective degradation of OG_{mix}. It was observed that the degradation of the BB had not started before the degradation of OG was completed and even after that BB degradation was very slow for both catalysts. It was assumed that the interaction of OG and BB in a mixed dye system led to a significantly faster and selective degradation of OG_{mix}. Even CoA-1100, which was less effective for the other tested dye systems, showed excellent degradation efficiency. Also, the degradation of BB as a single dye was slower than for all other dyes tested in this study, indicating that the tested catalysts were the least effective for the degradation of this dye.

Since the adsorption of all investigated dyes was negligible, the observed degradation efficiency for single dye degradation can be probably attributed to differences in the molecular structure of the dyes [28,29]. OG and RB are anionic dyes, while MB and BB are cationic. Besides, OG and BB are azo dyes, MB is a heterocyclic aromatic chemical compound, while RB is an anthraquinone dye. On the other hand, degradation in a dye mixture involves interactions and competition between dyes [30].

4. CONCLUSION

Oxone® induced catalytic oxidative degradation of Orange G (OG) was investigated using two structurally and texturally different cobalt-doped alumina catalysts (CoA-1000 - calcined at 1000 °C and CoA-1100 - calcined at 1100 °C). The catalysts were characterized by using scanning electron microscopy. The surface microstructure of the CoA-1000 catalyst showed plate-like formations of different sizes and the presence of white spherical particles of similar sizes. A more homogeneous morphology without plate formations was observed in the case of CoA-1100. The presence of $Co_3O_4/CoAl_2O_4$ phases at CoA-1000 was also recognized indirectly by applying the EDX technique.

Influences of temperature and initial pH value on the degradation efficiency of OG were followed. It was found that the reaction rate increased with the temperature increase both for CoA-1000 and CoA-1100. The highest degradation rate was obtained at 60 °C. The pseudo-first order kinetic model was proved to be the most applicable, and the activation energy was about 80 kJ mol^{-1} for both catalysts. It was also shown that the reaction rate was the highest at an initial pH 7 for both catalysts, but they can be used in a wide range of initial pH values. Effects of coexisting cations and anions on the degradation rate were investigated in an attempt to simulate the real situation in practice. It was shown that all non-metal redox cations (Ca^{2+}, Mg^{2+}, K^{+}, and Na^{+}) as well as anions: Cl^{-} and $H_2PO_4^{-}$ enhanced the OG degradation rate, while NO_3^{-}, $SO_4^{2-}$and HCO_3^{-} inhibited OG degradation. Apart from OG degradation, the degradation of three other dyes (Methylene blue, Remazol brilliant blue, and Basic blue 41) was also investigated. Both studied catalysts were found to be efficient in these reactions, but a better performance of CoA-1000 was noticeable for all investigated dyes. Such finding is the consequence of differences in the structural and textural properties of the two catalysts, but most importantly of different cobalt phases present.

In the end, degradation of dyes in three binary dye mixtures was tested showing that the investigated catalysts can be used in complex systems with more than one organic pollutant present in wastewater.

Supplementary material: Additional data are available electronically on the article page on the journal's website: www.ache-pub.org.rs/index.php/HemInd/article/view/1218, or from the corresponding author on request.

Acknowledgments: This research was financially supported by the Ministry of Science, Technological Development and Innovation of the Republic of Serbia (Contract No: 451-03-66/2024-03/200026).

REFERENCES

[1] Busca G. Structural, surface, and catalytic properties of aluminas. In: Jentoft F, ed. Advances in Catalysis, Norman, Oklahoma, USA, Elsevier Inc. 2014; 57: 2-412, ISSN 0360-0564; http://dx.doi.org/10.1016/B978-0-12-800127-1.00003-5

[2] Maldonado CS, De la Rosa JR, Lucio-Ortiz C, Hernández-Ramírez A, Castillón Barraza F, Valente J. Low concentration Fe-doped alumina catalysts using sol-gel and impregnation methods: The synthesis, characterization and catalytic performance during the combustion of trichloroethylene. *Materials.* 2014; 7: 2062-2086. http://dx.doi.org/10.3390/ma7032062

[3] Jiratova K, Beranek L, Properties of modified aluminas. *Appl Catal.* 1982; 2: 125-138. http://doi.org/10.1016/0166-9834(82)80196-6

[4] Matori KA, Wah LC, Hashim M, Ismail I, Mohd Zaid MH. Phase transformations of α-alumina made from waste aluminum via a precipitation technique., *Int J Mol Sci.* 2012; 13: 16812-16821 doi:10.3390/ijms131216812

[5] Gitzen WH. Alumina as a ceramic material; Wiley-American Ceramic Society, Columbus, OH, USA, 1970.

[6] Khattak AK, Afzal M, Saleem M, Yasmeen G, Ahmad R, Surface modifcation of alumina by metal doping, Colloid surf A 2000; 162: 99-106 https://doi.org/10.1016/S0927-7757(99)00218-6.

[7] Marinović S, Mudrinić T, Dojčinović B, Barudžija T, Banković P, Novaković T, Cobalt-doped alumina catalysts in catalytic oxidation of tartrazine induced by Oxone®. J Environ Chem Eng. 2021; 9: 106348 (8 pages). https://doi.org/10.1016/j.jece.2021.106348

[8] Jovanović A, Bugarčić M, Sokić M, Barudžija T, Pavićević V, Marinković A, Photodegradation of thiophanate-methyl under simulated sunlight by utilization of novel composite photocatalysts. *Hem Ind.* 2024. https://doi.org/10.2298/HEMIND230523004J

[9] Hu P, Long M, Cobalt-catalyzed sulfate radical-based advanced oxidation: A review on heterogeneous catalysts and applications. *Appl Catal.* 2016; 181: 103-117.http://dx.doi.org/10.1016/j.apcatb.2015.07.024

[10] Nfodzo P, Choi H, Triclosan decomposition by sulfate radicals: Effects of oxidant and metal doses. *Chem Eng J.* 2011; 174: 629-634.http://dx.doi.org/10.1016/j.cej.2011.09.076

[11] Zhou ZG, Du HM, Dai Z, Mu Y, Tong LL, Xing QJ, Liu SS, Ao Z, Zou JP, Degradation of organic pollutants by peroxymonosulfate activated by MnO2 with different crystalline structures: Catalytic performances and mechanisms. *Chem Eng J.* 2019; 374: 170-180. https://doi.org/10.1016/j.cej.2019.05.170

[12] Stevanović G, Jović-Jovičić N, Popović A, Dojčinović B, Milutinović-Nikolić A, Banković P, Ajduković M, Degradation of textile dyes by Oxone® activated by cobalt supported chitosan-derived carbon-smectite catalyst. *Sci Sinter.* 2024; https://doi.org/10.2298/SOS2304270375

[13] KulićMandić A, Bečelić Tomin M, PucarMilidrag G, Rašeta M, Kerkez Đ, Application of impregnated biocarbon produced from soybean hulls in dye decolorization. Hem Ind. 2021; 75: 307-320. https://doi.org/10.2298/HEMIND210427023K

[14] Ganesan S, Kokulnathan T, Sumathi S, Palaniappan A, Efficient photocatalytic degradation of textile dye pollutants using thermally exfoliated graphitic carbon nitride (TE-g-C3N4). Sci Rep. 2024; 14: 2284. https://doi.org/10.1038/s41598-024-52688-y

[15] Far HS, Hasanzadeh M, Najafi M, Rabbani M, Highly porous organoclay-supported bimetal-organic framework (CoNi-MOF/OC) composite with efficient and selective adsorption of organic dyes. Environ Sci Pollut Res. 2023; 30: 43714-43725

[16] https://doi.org/10.1007/s11356-023-25374-1

[17] Thao LT, Nguyen TV, Nguyen VQ, Phan NM, Ki Jae Kim, Huy NN, Dung NT, Orange G degradation by heterogeneous peroxymonosulfate activation based on magnetic MnFe2O4/α-MnO_2 hybrid, J Environ Sci. 2023; 124: 379-396 https://doi.org/10.1016/j.jes.2021.10.008.

[18] Zhang J, Zhua MCL, Activation of peroxymonosulfate by iron-based catalysts for orange G degradation: role of hydroxylamine. RSC Adv. 2016; 6: 47562-47569 https://doi.org/10.1039/C6RA07231C

[19] Wu M, Wang Y, Lu B, Xiao B, Chen R, Liu H, Efficient activation of peroxymonosulfate and degradation of Orange G in iron phosphide prepared by pickling waste liquor. Chemosphere. 2021; 269: 129398.https://doi.org/10.1016/j.chemosphere.2020.129398

[20] Yu B, Li Z, Zhang S, Zero-valent copper-mediated peroxymonosulfate activation for efficient degradation of azo dye Orange G. Catalysts. 2022; 12: 700. https://doi.org/10.3390/catal12070700

[21] Madihi-Bidgoli S, Asghari F, Cheraghi S, Hamidinia H, Shagerdi E, AsadnezhadS, UV/periodate and UV/chlorine for dye degradation and real wastewater treatment: a comparative study, Water Pract Technol. 2023; 18: 2453-2468.https://doi.org/10.2166/wpt.2023.160

[22] Li C, Huang Y, Dong X, Sun Z, Duan X, Ren B, Zheng S, Dionysiou DD, Highly efficient activation of peroxymonosulfate by natural negatively-charged kaolinite with abundant hydroxyl groups for the degradation of atrazine, ApplCatal B: Environ. 2019; 247: 10-23. https://doi.org/10.1016/j.apcatb.2019.01.079

[23] Zhou G, Xu Y, Zhang X, Sun Y, Wang C, Yu P, Efficient Activation of Peroxymonosulfate by Cobalt Supported Used Resin Based Carbon Ball Catalyst for the Degradation of Ibuprofen. Materials. 2022; 15:5003. https://doi.org/10.3390/ma15145003
[24] Li N, Wang Y, Cheng X, Dai H, Yan B, Chen G, Hou L, Wang S, Influences and mechanisms of phosphate ions onto persulfate activation and organic degradation in water treatment: A review, Water Res. 2022; 222: 118896. https://doi.org/10.1016/j.watres.2022.118896
[25] Sheng B, Huang Y, Wang Z, Yang F, AiL, Liu J,On peroxymonosulfate-based treatment of saline wastewater: When phosphate and chloride co-exist,RSC Adv.2018; 8: 13865. http://doi.org/10.1039/c8ra00600h
[26] Zhao X, Ana QD, Xiao ZY, Zhai SR, Shi Z, Seaweed-derived multifunctional nitrogen/cobalt-co doped carbonaceous beads for relatively high-efficient peroxymonosulfate activation for organic pollutants degradation, Chem Eng J. 2018; 353: 746-759. https://doi.org/10.1016/j.cej.2018.07.171
[27] Yuan R, Ramjaun SN, Wang Z, Liu J, Effects of chloride ion on degradation of Acid Orange 7 by sulfate radical-based advanced oxidation process: Implications for formation of chlorinated aromatic compounds, J Hazard Mater. 2011; 196: 173-179. https://doi.org/10.1016/j.jhazmat.2011.09.007
[28] Xu A, Wei Y, Zou Q, Zhang W, Jin Y, Wang Z, Yang L, Li X, The effects of nonredox metal ions on the activation of peroxymonosulfate for organic pollutants degradation in aqueous solution with cobalt based catalysts: A new mechanism investigation, J Hazard Mater. 2020; 382: 121081. https://doi.org/10.1016/j.jhazmat.2019.121081
[29] Lončarević D, Dostanić J, Radonjić V, ŽivkovićLj, Jovanović D, Simultaneous photodegradation of two textile dyes usingTiO2 as a catalyst, React Kinet Mech Cat. 2016; 118: 153-164. http://doi.org/ 10.1007/s11144-016-0990-0
[30] Lin KYA, Lin TY, Degradation of Acid Azo Dyes Using Oxone Activated by Cobalt Titanate Perovskite, Water Air Soil Pollut. 2018; 229:10. https://doi.org/10.1007/s11270-017-3648-2
[31] Verma S, Rao BT, Singh R, Kaul R, Photocatalytic degradation kinetics of cationic and anionic dyes using Au-ZnO nanorods: Role of pH for selective and simultaneous degradation of binary dye mixtures, Ceram Int. 2021; 47: 34751-34764.https://doi.org/10.1016/j.ceramint.2021.09.014

Fentonov tip oksidativne degradacije boje Orange G i binarnih smeša boja pomoću Oksona® aktiviranog katalizatorima na bazi aluminijum oksida dopiranih kobaltom

Sanja R. Marinović[1], Tihana M. Mudrinić[1], Marija J. Ajduković[1], Nataša P. Jović-Jovičić[1], Dimitrinka A. Nikolova[2], Predrag T. Banković[1] i Tatjana B. Novaković[1]

[1]Univerzitet u Beogradu-Institut za hemiju, tehnologiju i metalurgiju, Centar za katalizu i hemijsko inženjerstvo, Beograd, Srbija
[2]Institut za katalizu, Bugarske akademije nauka, Sofija, Bugarska

(Naučni rad)

Izvod

Dva kobaltom dopirana katalizatora na bazi aluminijum oksida, sa ra zličitim teksturalnim i strukturnim karakteristikama, dobijena su sol-gel postupkom sinteze, nakon koje su uzorci žareni na tempreturi od 1000 °C odnosno 1100 °C. Dobijeni materijali su ispitani kao katalizatori u procesu degradacije anjonske tekstilne boje *Orange* G (OG) uz korišćenje Oksona kao prekursora sulfatnih anjon radikala, koji su glavna oksidativna vrsta. Ispitan je uticaj temperature i početnog pH na efikasnost degradacije, i uočeno je da porast temperature povećava brzinu reakcije. Maksimalna efikasnost degradacijeje dobijena na 60 °C. Primenjeni su različiti kinetički modeli i pokazalo se da kinetički model pseudo-prvog reda najbolje opisuje kinetiku ispitanog procesa. Takođe je za oba katalizatora utvrđeno da je optimalna vrednost pH za ispitivanu reakciju u oblasti blizu neutralne. Koegzistirajući katjoni (Ca^{2+}, Mg^{2+}, K^+ and Na^+) i anjoni Cl^- and $H_2PO_4^-$ su ubrzavali degradaciju OG, dok su je anjoni NO_3^-, SO_4^{2-} i HCO_3^- usporavali. Katalizatori su se pokazali efikasnii u degradaciji boja: metilensko plavo, osnovno plavo 41 i boje "Remazol brilliant blue", kao i u degradaciji boja u binarnim smešama. Ipak, razlike u strukturnim i teksturalnim svojstvima su uticale na razlike u katalitičkoj efikasnosti ova dva katalizatora.

Ključne reči: sol-gel aluminijum oksid; anjonske i katjonske boje; peroksimonosulfat; napredni oksidativni procesi; simultana degradacija bojai